

A PETROLOGIC STUDY OF AFAR TRIANGLE BASALTS OCEANS IN AFRICA?  
Is New Oceanic Crust Forming in East Africa? The Epic Search for New Oceanic Crust in  
the Afar Triple Junction!

By  
Mike Bagley, Sean Bryan, Dudley Loew, and Ellen Schaal

Bereket Haileab

Petrology

Spring, 2004

## **INTRODUCTION**

This study examines basalts from the Afar triangle region of Eastern Africa. The Afar region is located southwest of the Red Sea in northeastern Ethiopia and eastern Eritrea (Fig. 1). Previous petrologic studies in the Afar have shown the presence of heterogeneous sources of magmas erupting in this area, and have disputed the nature of the Afar crust (Barberi et al., 1975; Bizouard et al., 1980; Barrat et al., 1998). The results from several different analyses in this study suggest that there is new oceanic crust forming in the Afar region in East Africa, of E-MORB like composition. For this paper, basalt samples from several locations in the Eritrean part of the Afar region were analyzed using a petrographic microscope, SEM (Scanning Electron Microscopy), and XRF (X-Ray Fluorescence) to obtain their mineralogy, major element, and minor/trace element compositions, respectively. The data was graphed and compared with standard magma chemical compositions for different melt sources in order to determine the nature of the basalts forming at the Afar triple junction spreading center.

## **GEOLOGIC SETTING**

The Afar region of eastern Africa encompasses about 200,000 km<sup>2</sup> and is mostly below sea level, reaching a minimum of 160 m below sea level (Barberi et al., 1974).

The Afar depression is one of the most unique geological settings on the Earth today; it represents the only modern example of continental rifting ~~at~~ an active triple-junction, where three ~~spreading centers or~~ rift zones meet (with approximately 180 degree angles) at a point from which the three surrounding adjacent tectonic plates are diverging. □ Two

of the three rift arms extend-emanating from the Afar triangle are represented by the Gulf of Aden and the Red Sea; spreading created these young, narrow seas and active rifting continues to widen them into new ocean basins.□The third arm of the triple junction is the East African Rift system, which runs north-south and was formed by the separation of the African and Arabian tectonic plates beginning over 35 million years ago. The East African Rift Valley ~~is thought to be~~ may represent a failing rift that will not develop into a new ocean basin; the African rift is only spreading at a rate of 6mm/yr in contrast to the 2 cm/yr divergence along the other two rift arms ~~(CITATION)~~.□The Afar region of East Africa rests ~~at~~ in the middle of the triple-junction spreading center (Fig 2). The region encompasses about 200,000 km<sup>2</sup> and is mostly below sea level, reaching a minimum of 160 m below sea level (Barberi et al., 1975). ~~The Afar region~~ and shows many landforms associated with the tectonic spreading of the triple junction, including (step) faults, cinder cone volcanoes, and graben features. Because the Afar region offers a rare example of continental rifting and an active triple junction, along with the possible development of new oceanic crust, it is ~~the combination of these features makes the Afar region as~~ one of the most petrologically and tectonically and petrologically significant settings on Earth.

## **GEOLOGIC SETTING**

### **SAMPLE LOCATIONS**

In this study, basalt samples from six locations in the Afar triangle region ~~of East Africa~~ were analyzed. Samples ASB-32, GAL-11, EE-29, BLL-24 came from sites on the rift valley floor, ~~which is mostly below sea level~~ (see map, Ffig. 1#). In contrast, samples SD-218B and TIM-174 were taken from two sites farther to the northwest, in the

highlands. These two samples were still collected from flood basalts associated with the East African Rift, but they might be expected to differ in chemical composition from the more recent basalts of the rift valley floor because of their distinct geologic setting.

~~Thin sections~~ from each of these locations ~~were~~ studied ~~under~~ under the petrographic microscope and used for microprobe analysis. In a different study by Bereket Haileab, the. In a different study at Carleton College, whole rock geochemistry was measured for the same rock samples, using XRF analysis to obtain ~~were also analyzed for trace element and stable isotope data, and isotope analysis was done at ACT Labs.~~ and this data was analyzed in this study using the Icpet program...

## METHODS

Although not, as it turns ~~ed~~ out, key to ~~our~~ the results of this study analysis, the six thin sections ~~we did direct experimental work on~~ were analyzed provided some result using scanning electron microscopy, and ~~more importantly~~ provided an interesting opportunity to use and learn about ~~the Scanning Electron Microprobe (SEM)~~ at the University of Minnesota. ~~Each thin section came from a different location in the Eritrean/Ethiopian Afar~~ First the samples were our primary contribution to their creation was to polished down to 2 microns them for in preparation for SEM preparation. Next, the ~~Once polished to an arbitrary degree, we took our~~ sections were taken to the U of

~~M~~University for probing, where Ellery Frahm assisted ~~u~~ and coated with carbons in carbon coating them. This process is very important in SEM analysis to ground the samples and prevent electron buildup. Using the JEOL 8900 “Super Probe” Electron Probe Microanalyzer, standards were run for each of the minerals to be analyzed, so that the machine could use the parameters for the “pure” pyroxenes to scan for the pyroxenes in the thin sections. That minor preparation was followed by the major one of “teaching” the machine what we were looking for by having it probe standards for each of our minerals, so that it could calculate correlations and deviations between “pure” pyroxenes and our pyroxenes. Finally, ~~we installed~~ the samples were loaded in the SEM, ~~the evacuated the~~ analysis chamber was evacuated, ~~and started selecting~~ points were selected on each thin section slide for analysis later probing.

~~P~~We were attempting to probing was performed to measure for the compositions of three minerals: plagioclase, pyroxene, and ilmenite. Each has ~~d~~ different characteristics in the electron backscatter imaging that ~~were~~ used to “visually” scan the samples and select points. Plagioclase, ~~it turns out~~, is not particularly reflective of electrons, and so appears almost black, pyroxenes are an intermediate grey color, and ilmenites show up ~~are~~ almost white. This is due to a correlation between reflectivity and metallic content; ~~thus, t-~~ ilmenite,  $\text{FeTiO}_3$ , is clearly going to be more reflective ~~of~~ electrons than plagioclase,  $(\text{Ca,Na})\text{Al}_2\text{Si}_2\text{O}_8$ . Approximately ~~In any case, we selected~~ about 100 points ~~for~~ each mineral were selected for probe analysis, distributed approximately equally among the slides. In many cases, ~~we set several many~~ points or transects were taken ~~on~~ across a single grains, to test for zoning, or chemical differences ~~between~~ from their cores and ~~to~~ their rims ~~from reactions with surrounding material~~.

~~When we actually ran our samples, the microprobe was set at conditions included an accelerating voltage of 15 kV; and a the beam diameter was of 5 microns. This was the beam diameter at the sample surface; the interaction volume was probably more like 6 or 7 microns in diameter (pers. comm. Frahm, 2004).~~

~~Several days after performing our microprobe analysis, we received our results, and it became clear that we had further work to do on it before attempting to derive conclusions from it. As it turned out, illmenite was not the only mineral in the our thin sections to appear almost white in electron backscatter, with small, elongate grains. GarnetOlivine, another highly metallic mineral, was also present, and many of the points we set to analyze illmenite grains turned out to be located on garnetsolivines, making most rendering much of the our illmenite data worth unusable less. Fortunately, much good The junk data was obtained for the our pyroxenes and plagioclase grains ioclases was much smaller in extent, luckily, Cleaning and in order to clean these two data sets involved, were ordered sorting them in Excel by their chemical totals (which ranged from less than 50 50 percent to more than 105 5 percent), and started eliminating all data points with less than 94 or greater than 102 percent chemical total data points. We determined the range of totals we would accept based on the volatiles that could possibly have been present in the minerals, which would not be measured in our analysis, and instead showed up as bulk mineral chemistry adding up to less than 100%. The literature (CITATION) gave us surprisingly high numbers for possible volatile content. Next, the data was sorted by silica content, and all measurements with less than 33% or greater than 63% silica were eliminated. Finally, the pyroxene data was sorted by aluminum content, and all measurements with less than~~

~~0.07% or greater than 27% were also eliminated. These ranges for acceptable silica and aluminum content were taken from Deer et al. (151-153). -so we ended up allowing a relatively wide range of totals.~~

~~The rest of our data gathering and~~ Most of the remaining data analysis ~~took place primarily in the context~~ was performed using ~~of the~~ igneous petrology analysis software ~~appropriately nam~~ appropriately named Igpet. Given a properly ~~It can take a properly~~ formatted spreadsheet of chemical and isotopic data for a suite of rocks, ~~and then this program can~~ display them ~~on any of~~ a huge range of diagrams that have been developed for classifying and analyzing igneous rocks. ~~We looked at~~ Examples of useful diagrams produced by Igpet include ~~everything from REE spider diagrams for isotopes (Fig. \_\_\_\_\_) to~~ AFM ternary diagrams for whole rock major element ~~pyroxene~~ compositions (Fig. \_\_\_\_\_) ~~and~~ rare earth element spider diagrams for isotopes.

~~Not only does Igpet do this possibly tedious task automatically, allowing us to look at an overwhelming array of possibilities in displaying our data (and that derived from the isotope analysis provided to us by Bereket Haileab) in a short time. It even provides the citations for each graphing technique, allowing quick reference to the original work, if problems are encountered.~~

## **RESULTS AND DISCUSSION**

### **Petrography**

An examination of the thin sections under a petrographic microscope yielded some interesting differences between the six basalt samples in this study. All samples ~~appear unmetamorphosed but~~ contain significant alteration and secondary minerals;

olivine rims have altered to iddingsite and plagioclase has altered to analcime in some samples (TIM-174 and SD-218B), and many vesicles are filled with calcite or zeolites. In addition, the samples' mineralogical composition shows similar percentages of plagioclase, ~~olivine, ortho and orthopyroxene, and Fe-Ti oxides~~ (Table 1). Despite these similarities, there are ~~a few significant~~ differences in the original mineralogy of these rocks from the Afar. Samples BLL-24, GAL-11, TIM-174, and SD-218B contains olivine phenocrysts that are significantly larger than the surrounding minerals, including the smaller crystals of olivine. These were presumably the first to crystallize, perhaps under different magmatic conditions than the surrounding matrix of smaller plagioclase, pyroxene, and olivine crystals. In contrast, the largest phenocrysts in samples EE-29 and ASB-32 are twinned and zoned plagioclase crystals, ~~whereas the and the~~ surrounding olivine and plagioclase crystals are small in comparison. In addition, the two highlands samples, TIM-174 and SD-218B, contained a couple of notable mineralogical differences from the Afar samples. These rocks contained a significant percentage of analcime, probably due to the alteration of plagioclase; this could reflect the greater age, and hence more exposure to changing chemical conditions, of these rocks. The thin sections from the highlands also contained significantly fewer vesicles than the rift valley samples, which all contained about 10% empty space and also vesicles filled with calcite. Perhaps this points to a difference in volatile content between the magmas of the two locations.

**Table 1: Petrography data**~~Both samples contain orthopyroxene oikocrysts, which surround the small plagioclase laths.~~

Sample Name	Thin Section	Plagioclase	Pyroxene	Olivine	Fe-Ti Oxides	Analcime	Calcite
<u>BLL-24</u>	<u>GPT-31</u>	<u>50%</u>	<u>15%</u>	<u>12%</u>	<u>3%</u>	<u>□</u>	<u>10%</u>
<u>□</u>	<u>□</u>	<u>□</u>	<u>□</u>	<u>□</u>	<u>□</u>	<u>□</u>	<u>□</u>
<u>□</u>	<u>□</u>	<u>□</u>	<u>□</u>	<u>□</u>	<u>□</u>	<u>□</u>	<u>□</u>



<u>GAL-11</u>	<u>GPT-40</u>	<u>48%</u>	<u>28%</u>	<u>6%</u>	<u>5%</u>	<u>0</u>	<u>0</u>
<u>0</u>	<u>0</u>	<u>0</u>	<u>0</u>	<u>0</u>	<u>0</u>	<u>0</u>	<u>0</u>
<u>0</u>	<u>0</u>	<u>0</u>	<u>0</u>	<u>0</u>	<u>0</u>	<u>0</u>	<u>0</u>
<u>EE-29</u>	<u>GPT-36</u>	<u>47%</u>	<u>15%</u>	<u>8%</u>	<u>8%</u>	<u>0</u>	<u>12%</u>
<u>0</u>	<u>0</u>	<u>0</u>	<u>0</u>	<u>0</u>	<u>0</u>	<u>0</u>	<u>0</u>
<u>0</u>	<u>0</u>	<u>0</u>	<u>0</u>	<u>0</u>	<u>0</u>	<u>0</u>	<u>0</u>
<u>ASB-32</u>	<u>GPT-17</u>	<u>50%</u>	<u>18%</u>	<u>5%</u>	<u>8%</u>	<u>0</u>	<u>8%</u>
<u>0</u>	<u>0</u>	<u>0</u>	<u>0</u>	<u>0</u>	<u>0</u>	<u>0</u>	<u>0</u>
<u>0</u>	<u>0</u>	<u>0</u>	<u>0</u>	<u>0</u>	<u>0</u>	<u>0</u>	<u>0</u>
<u>TIM-174</u>	<u>GPT-77</u>	<u>55%</u>	<u>15%</u>	<u>10%</u>	<u>5%</u>	<u>6%</u>	<u>0</u>
<u>0</u>	<u>0</u>	<u>0</u>	<u>0</u>	<u>0</u>	<u>0</u>	<u>0</u>	<u>0</u>
<u>0</u>	<u>0</u>	<u>0</u>	<u>0</u>	<u>0</u>	<u>0</u>	<u>0</u>	<u>0</u>
<u>SD-218B</u>	<u>GPT-66</u>	<u>50%</u>	<u>15%</u>	<u>15%</u>	<u>3%</u>	<u>15%</u>	<u>0</u>
<u>0</u>	<u>0</u>	<u>0</u>	<u>0</u>	<u>0</u>	<u>0</u>	<u>0</u>	<u>0</u>
<u>0</u>	<u>0</u>	<u>0</u>	<u>0</u>	<u>0</u>	<u>0</u>	<u>0</u>	<u>0</u>

Table 1 (Continued)

<u>Sample Name</u>	<u>Other</u>	<u>Notes:</u>	<u>0</u>	<u>0</u>	<u>0</u>	<u>0</u>	<u>0</u>
<u>BLL-24</u>	<u>vesicles and</u>	<u>Relatively large olivine phenocrysts, olivine rims altering to iringsite, smaller</u>					
<u>0</u>	<u>other empty</u>	<u>plagioclase laths, tiny anhedral crystals of OPX with no visible oikocrysts,</u>					
<u>0</u>	<u>space 8%</u>	<u>calcite filling some round vesicles and other spaces in the mineral structure</u>					
<u>GAL-11</u>	<u>vesicles and</u>	<u>Relatively large olivine phenocrysts, olivine almost entirely altered to iringsite,</u>					
<u>0</u>	<u>other empty</u>	<u>oikocrysts of OPX (18%) and CPX (10%) surround smaller plagioclase laths</u>					
<u>0</u>	<u>space 10%</u>	<u>0 0 0 0 0 0 0</u>					
<u>EE-29</u>	<u>vesicles and</u>	<u>Relatively large plagioclase phenocrysts (some zoned and twinned), olivine rims</u>					
<u>0</u>	<u>other empty</u>	<u>altering to iringsite, OPX oikocrysts surround smaller plagioclase laths,</u>					
<u>0</u>	<u>space 10%</u>	<u>a high percentage of calcite in the rock - vesicles and other spaces</u>					
<u>ASB-32</u>	<u>vesicles and</u>	<u>Relatively large plagioclase phenocrysts (some zoned &amp; twinned), smaller plagioclase</u>					
<u>0</u>	<u>other empty</u>	<u>laths cut through them, olivine rims altering to iringsite, OPX oikocrysts surround</u>					
<u>0</u>	<u>space 10%</u>	<u>smaller plagioclase laths, secondary minerals such as calcite fill some vesicles</u>					
<u>TIM-174</u>	<u>chlorite 6%</u>	<u>Relatively large olivine phenocrysts almost entirely altered to iringsite,</u>					
<u>0</u>	<u>0</u>	<u>a significant proportion of chlorite in this rock, relatively small OPX crystals</u>					
<u>0</u>	<u>0</u>	<u>surround plagioclase laths but no large OPX oikocrysts, plagioclase altering to analcime</u>					
<u>SD-218B</u>	<u>zeolites</u>	<u>Large and small olivine phenocrysts, large olivines have good crystal form,</u>					
<u>0</u>	<u>one vesicle</u>	<u>olivine rims altering to iringsite and chlorite in places, OPX oikocrysts surround</u>					
<u>0</u>	<u>0</u>	<u>plagioclase, plagioclase laths are all very small, plagioclase altering to analcime</u>					

**GEOCHEMISTRY**

**Stable Isotope Data**

Samples from four of the locations in the Afar region were tested for stable isotope data, providing ratios for lead, strontium, and neodymium isotopes ( $^{206}\text{Pb}/^{204}\text{Pb}$ ,  $^{207}\text{Pb}/^{204}\text{Pb}$ ,  $^{143}\text{Nd}/^{144}\text{Nd}$ , and  $^{87}\text{Sr}/^{86}\text{Sr}$ ) (Table 2).

**Table 2:**

<u>Sample Name</u>	<u><math>\{^{206}\text{Pb}/\{^{204}\text{Pb}\}</math></u>	<u><math>\{^{207}\text{Pb}/\{^{204}\text{Pb}\}</math></u>	<u><math>\{^{143}\text{Nd}/\{^{144}\text{Nd}\}</math></u>	<u><math>\{^{87}\text{Sr}/\{^{86}\text{Sr}\}</math></u>
<u>BLL-24</u>	<u>18.596</u>	<u>15.546</u>	<u>0.512948</u>	<u>0.703802</u>
<u>EE-29</u>	<u>18.467</u>	<u>15.567</u>	<u>0.51288</u>	<u>0.704017</u>
<u>GAL-11</u>	<u>18.76</u>	<u>15.573</u>	<u>0.512882</u>	<u>0.703629</u>
<u>TIM-174</u>	<u>18.344</u>	<u>15.533</u>	<u>0.512974</u>	<u>0.703006</u>

\_\_\_\_\_ The program Igpct was used to graph the various stable isotope ratios against each other, to see where samples BLL-24, EE-29, GAL-11, and TIM-174 they fell in relation to 'mantle component' fields for melt-tectonic origin of basaltic rock types. -as previously determined by? The four samples, EE 29, GAL 11, BLL 24, and TIM 174, plotted in a fairly tight cluster (see fig.s \_\_\_\_\_), with sample TIM 174 typically plotting farthest from the rest of the cluster. Since sample TIM 174 is from the highlands northwest of the rift valley floor, one might expect a somewhat different chemical composition for the basalts in this area of the Afar. According to \*\*\*, these northeastern rocks are older flood basalts, and thus may represent the earlier stages of rifting in the Afar.

\_\_\_\_\_ Unfortunately, the four samples mostly plot in a cluster outside of the fields indicating probable melt-tectonic origin, as graphed in Igpct (Fig.s 3-5). This may be due to error in the stable isotope measurements or conservative size of the mantle component fields represented in Igpct's version of the comparative stable isotope ratio graphs.

However, the samples do fall plot close enough to these mapped within these mapped

fields that they fit, given a certain degree of error. The four samples consistently plot in a cluster very near the PREMA (prevalent mantle) and MORB fields (Fig.s 3-5). This result...

—————Sample TIM-174 from the highlands falls neatly within the MORB field on the graph of  $^{87}\text{Sr}/^{86}\text{Sr}$  verses  $^{206}\text{Pb}/^{204}\text{Pb}$  ratios (Fig. 4). However, it falls within the PREMA field on the  $^{143}\text{Nd}/^{144}\text{Nd}$  verses  $^{206}\text{Pb}/^{204}\text{Pb}$  plot (Fig. 5). These two fields plot very close to one another, and the fact that a single data point can fall within both on different isotope graphs points to the idea that—and so this discrepancy probably reflects the error in the data. On the other hand, it may simply demonstrate how chemical variation in nature sometimes defies the divisions of classification systems.

## **DISCUSSION**

### **Stable Isotope Data**

—————Although the four samples, BLL-24, EE-29, GAL-11, and TIM-174, plotted in a fairly tight cluster on the stable isotope ratio graphs with mantle component fields (Fig.s 3-5), sample TIM-174 typically plotted farthest from the rest of the cluster. Since sample TIM-174 is the one sample from the highlands northwest of the rift valley floor in this set, one might expect a somewhat different chemical composition for the basalts in this area. These northwestern rocks are older flood basalts, and thus may represent the earlier stages of rifting in the Afar (pers. comm. Haileab, 2004).

does not always perfectly follow the observed average trends used for classification of rocks.

### **Major Element Data**

Major element weight percentages for the whole rock as well as for pyroxene and plagioclase were analyzed using Iqpet. An AFM diagram, constructed from the whole rock major element geochemistry, indicates that these rocks are unevolved tholeiitic basalts (Fig. 6#). These results suggest that the samples represent the beginning of the formation of oceanic crust in the Afar Depression. A trivariant plot of Na, Ca and K oxides was constructed from the plagioclase major element data (Fig. 7#). This plot shows the majority of the samples plotting near the middle of the left limb of the triangle; indicating very little ~~k~~K-feldspar, and slightly more ~~a~~Anorthite than ~~a~~Albite. The pyroxene major element data was also plotted on a tri-variant diagram of Mg, Ca and Fe oxides (Fig. 8#). The pyroxene samples plot in two cluster-groups, one near the top of the triangle and one near the middle. The samples contain nearly equal concentrations of magnesium and iron, but the first group is more calcium rich than the second.

### **MELTS Analysis**

The Minerals and Melts server (<http://penmelts.ess.washington.edu>) was used to analyze the major element data obtained from microprobe as well as XRF processing of ~~each o~~f the rock samples. MELTS was designed by Mark Ghiorso at the University of Chicago and others; it functions to provide the thermodynamic properties of mineral end-~~u~~members and solid solutions as well as calculate the phase equilibria of magmatic systems.

The MELTS Java Applet was used to determine liquidus temperatures for each of the rock samples. Weight % oxides from the whole rock XRF analysis were entered into the applet and the pressure was specified. Table 3# shows the resulting liquidus temperatures at pressures of 10 kbar, 1 kbar and 1 bar. These temperatures are

reasonable values for the basaltic samples (pers. comm. Haileab, 2004). There is no clear trend or grouping between the different samples.

Table 3#	Liquidus Temperature (degrees C)		
Sample	10 kbar	1 kbar	1 bar
<b>BLL-24</b>	1373.83	1235.06	1228.81
<b>ASB-32</b>	1351.86	1260.16	1253.52
<b>EE-29</b>	1364.75	1257.53	1251.57
<b>GAL-11</b>	1354.88	1230.37	1223.44
<b>SD-218B</b>	1368.16	1211.52	1204.59
<b>TIM-174</b>	1341.11	1246.97	1240.04

The plagioclase weight % oxides, obtained from the microprobe analysis, were entered into the MELTS Supplemental Mineral Calculator. The Mineral Calculator was used to convert the weight % oxides to mole fractions of the feldspar end-members: aAlbite, aAnorthite and sSanidine (Table 4#). The samples may be divided into two groups according to their fractions of aAlbite and aAnorthite: BLL-24, ASB-32, EE-29 and GAL-11 are all between 0.31 – 0.34 Ab and 0.65 – 0.68 An; whereas, SD-218B and TIM-174 have 0.42 – 0.44 Ab and 0.52 – 0.55 An. This division is appropriate and may be related to the locations where the samples were taken: again, sites n. SD-218B and TIM-174 are located in the highland mountains to the northeast of the rift and the others are from the lowlands close to the Red Sea (see location map, Fig. 1). t, presumably on continental crust, whereas, the rest of the samples are from the lowlands close to the Red Sea, probably on oceanic crust (see location map).

<b>Table 4# Mole Fractions of Feldspar End-members from Wt % Oxides</b>				
<b>Sample</b>	<b>Albite</b>	<b>Anorthite</b>	<b>Sanidine</b>	<b>Notes</b>
<b>BLL-24</b>	0.313261	0.674109	0.01263	Avg of 16 data pts
<b>ASB-32</b>	0.336859	0.655479	0.007663	Avg of 15 data pts
<b>EE-29</b>	0.316745	0.676309	0.006946	Avg of 20 data pts
<b>GAL-11</b>	0.336732	0.652248	0.011019	Avg of 15 data pts
<b>SD-218B</b>	0.426031	0.527452	0.046517	Avg of 4 data pts
<b>TIM-174</b>	0.43395	0.549424	0.016626	Avg of 10 data pts

The microprobe pyroxene data were also analyzed using the Mineral Calculator (Table 5#). The fractions of the various end-members vary widely from sample to sample, and no clear trends are apparent. The presence of Jadeite, however, may indicate that some pyroxenes formed at depth (pers. comm. Haileab, 2004). There seems to be a lot of error in the microprobe pyroxene data, which may be a result of misidentification of pyroxenes.

<b>Table 5 Mole Fractions of Pyroxene Endmembers from Wt % Oxides</b>				
<b>Sample</b>	<b>Diopside</b>	<b>Clinoenstatite</b>	<b>Hedenburgite</b>	<b>Alumino-buffonite</b>
<b>BLL-24</b>	-0.076419	0.074128	0.076451	0.478382
<b>ASB-32</b>	0.177431	0.191349	0.308481	0.229786
<b>EE-29</b>	0.07818	0.474892	0.00077	0.345992
<b>GAL-11</b>	0.446781	0.217616	0.74349	0.239579

<b>SD-218B</b>	-0.070676	0.039754	0.024592	0.63484
<b>TIM-174</b>	-0.004187	0.05764	0.09002	0.564696

	<b>Buffonite</b>	<b>Esseneite</b>	<b>Jadeite</b>	Notes
<b>BLL-24</b>	-0.451026	0.451798	0.446686	Avg of 5 data pts
<b>ASB-32</b>	-0.124966	0.128082	0.089837	Avg of 11 data pts
<b>EE-29</b>	-0.253144	0.329372	0.023939	Avg of 12 data pts
<b>GAL-11</b>	-0.187989	0.18874	0.020923	Avg of 13 data pts
<b>SD-218B</b>	-0.629341	0.62959	0.371241	Avg of 9 data pts
<b>TIM-174</b>	-0.541802	0.542711	0.290921	Avg of 7 data pts

### Comparison to Erta’Ale volcanics

Using *Igpet*, the isotope and trace element geochemistry results were compared to a study by Barrat et al. (1998) on volcanics from the Erta’Ale range in Ethiopia using *Igpet*. In general, the isotopes and trace elements from the Erta’Ale volcanics plot very closely to those of this study. Plots of Sr vs. Nd, Pb vs. Sr, and Pb vs. Nd isotopes show the two sets of points plotting in a tight cluster near the PREMA and MORB fields (Figs. 3#, 4# & 5#). In the plots of Pb vs. Sr and Pb vs. Nd, there is a slight differentiation between the two sets of points; however they are still very close together. The rare earth element concentrations plot together between 10 and 100, with the exception of four of the Erta’Ale samples, which are more enriched in the light REEs (Fig. 9#). The more enriched samples are intermediate to felsic volcanics. A tri-variant plot of La, Y, and Nb shows most points from this study falling within the E-MORB field, and from Barrat et al

(1998), falling within the Alkaline Intercontinental rifts and E-MORB fields (Fig. 10#); the two of the samples from this study which depart from the main cluster and are more enriched in Y are SD218B and TIM-174. A plot of Nb/Y vs. Zr/TiO<sub>2</sub> reveals that several of the samples from this study are depleted in Zr (Fig. 11#). The samples from Erta'Ale plot range from Alkali Basalt to Trachyte, while the samples from this study plot within the Basalt to Alkali Basalt range (Fig. 11#).

~~Barrat et al. (1998) argue that two distinct mantle sources, a depleted MORB and a HIMU OIB type, are responsible for the genesis of the Erta'Ale basalts. The findings of this study support this conclusion. The trace element and isotope chemistry indicate a source that is more enriched than the typical MORB, but less enriched than OIB type basalts. The result gives an EMORB type signature.~~

#### Dudley's section Rare Earth Elements and Mantle Melt Origins

A typical mid-oceanic ridge basalt (MORB) is an olivine tholeiite, with low K<sub>2</sub>O (<0.2%) and low TiO<sub>2</sub> (<2.0%) when compared to most other basalts. MORBs, however, are not uniform and display a range of trace-major element chemical compositions. However, the range is still considerably more restricted than most petrogenetic associations (Winter, p252)<sup>+</sup>. Because the range is so minute, rare earth elements, and not major element compositions, are used to distinguish between different types of MORBs. The Rare Earth Element technique is of great use in determining the origin of melts, and thus the similarities or differences between the varieties of oceanic basalts and the Afar basalts. ~~will be used to determine if the Afar region is producing oceanic or continental crust.~~

---

<sup>+</sup>Winter, pg. 252



After the plotting the Rare Earth Elements (REE) diagram of the four rift valley samples, it appears that all of them plotted very closely to one another. When looking at the composition of the rift valley samples, they had an average La of about 60 and Yb of about 20 on the rock/chondrite scale (Fig. 12). Comparing the four rift valley samples to the highland samples, there is a significant difference in REE trends between the two different locations. While the rift valley samples had an average La of about 60, the highland samples had a La average of around 25 on the rock/chondrite scale (Fig 12). While the samples from the valley and highlands have similar concentrations of heavy rare earth elements (Yb of about 20), the rift valley samples clearly have higher concentrations of light rare earth elements (LREE) as compared to the highland samples. Thus, the samples from the Afar valley are enriched in light rare earth elements.

In addition, the six basalt samples were plotted on three spider diagrams, normalized to N-MORB, E-MORB, and OIB values (Figs. 13-15). Experimental data trends that closely match the trend to which they were normalized should plot close to a flat line at 1 on the y-axis. The samples from the Afar seem to plot closest to 1 on the graph where they have been normalized to E-MORB, and thus, most closely match with experimentally determined enriched mid-ocean ridge basalt values (Fig. 14).

## **CONCLUSIONS**

Analysis of the basalt thin sections with the petrographic microscope revealed some mineralogical distinctions between the samples from different locations; the highland samples show more alteration (in correspondence with their greater age and presumed longer time of exposure), and the Afar valley samples tend to contain more vesicles, perhaps indicating a more volatile rich melt. Graphing the various stable

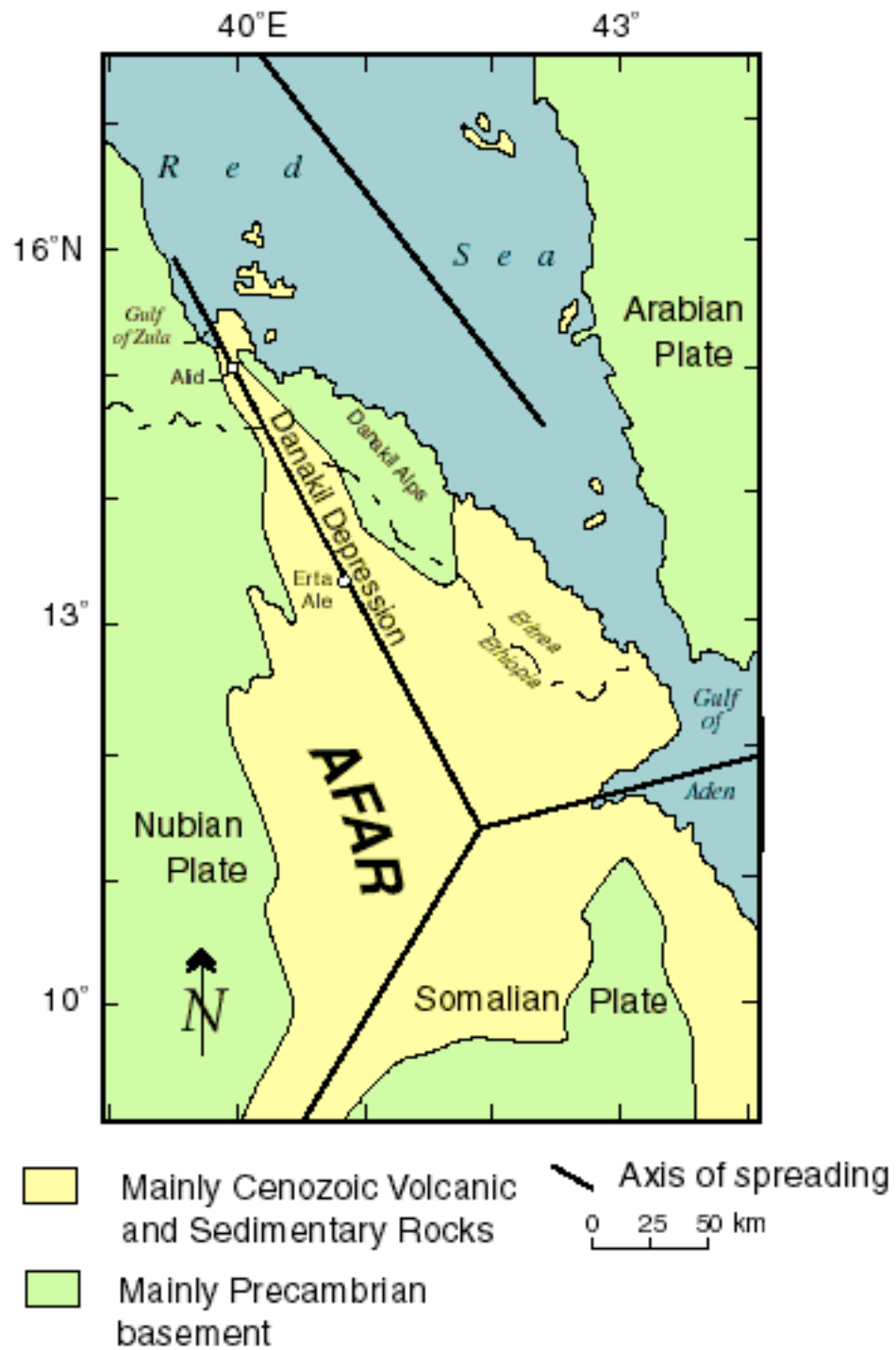
isotope ratios against each other, the data for the different sample locations showed a very similar isotopic signature. However, the TIM-174 sample from the highlands plots farthest from the cluster, consistent with its distinct geologic setting. The division of the samples into two clusters according to their relative fractions of albite and anorthite in the MELTS calculations also fits with the division between the two sample locations, rift depression and highlands. In addition, the stable isotope ratio graphs indicate all samples cluster within error of the MORB and PREMA mantle component fields, reservoirs common in ocean volcanics. The AFM diagram of whole rock major element data indicates the Afar samples are unevolved tholeiitic basalts (Fig. 6), and thus suggests that the samples could represent the beginning of the formation of oceanic crust in the Afar Depression.

In their article, Barrat et al. (1998) argue that two distinct mantle sources, a depleted MORB and a HIMU OIB-type, are responsible for the genesis of the Erta' Ale basalts. Because the data from this study fit so well with the Barrat et al. (1998) data set (Fig. 3), the findings of this study support their conclusion. The trace element and isotope chemistry indicate a source that is more enriched than the typical MORB, but less enriched than OIB type basalts; the result is an E-MORB type signature. The rare earth element data shows that the younger basalts of the rift valley floor are more enriched in light rare earth elements, when compared with the older flood basalts from the highlands. This suggests that the mantle source that is producing the rift valley rocks comes from a deeper mantle source that is enriched in LREE. This also suggests that although the highland and rift valley samples are relatively near each other, they do not necessarily come from the same combination of mantle sources, and there are, or have been through

time, heterogeneous or distinct mantle melt sources beneath eastern Africa. Finally, the rare earth element data shows that, despite the differences between the valley and highlands samples, the six Afar samples most closely match with experimentally determined E-MORB values (Fig. 14). Therefore, the results from several separate analyses support the conclusion that there is indeed new oceanic crust forming in the Afar region in East Africa, of E-MORB like composition.

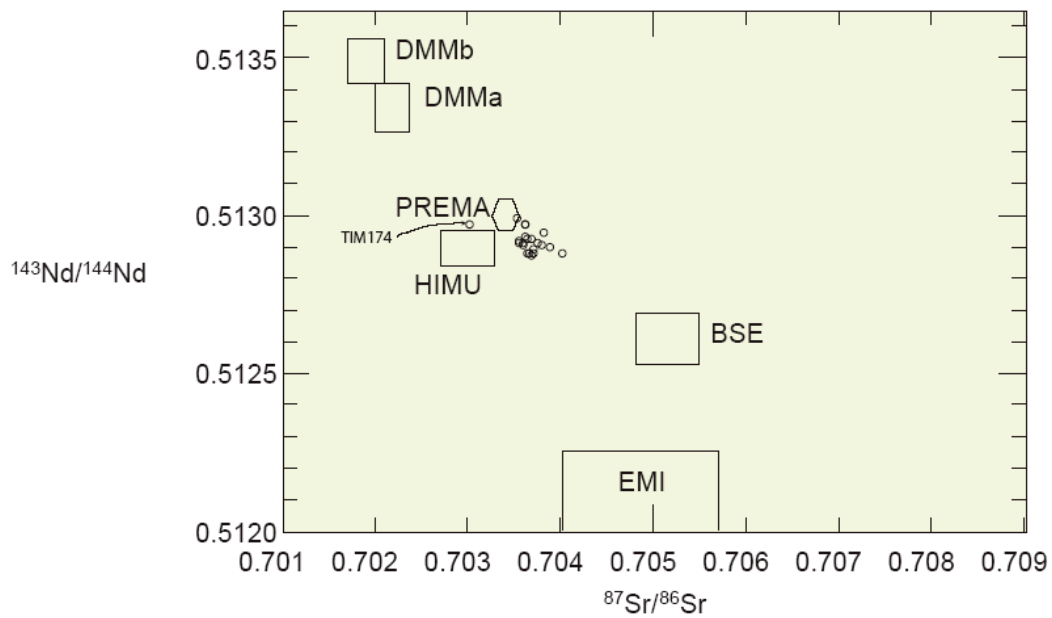


**Figure 1:** Map of the Afar region, East Africa. Locations for valley floor samples ASB-32, GAL-11, EE-29, and BLL-24, as well as highlands samples SD-218B and TIM-174 are indicated with red arrows.

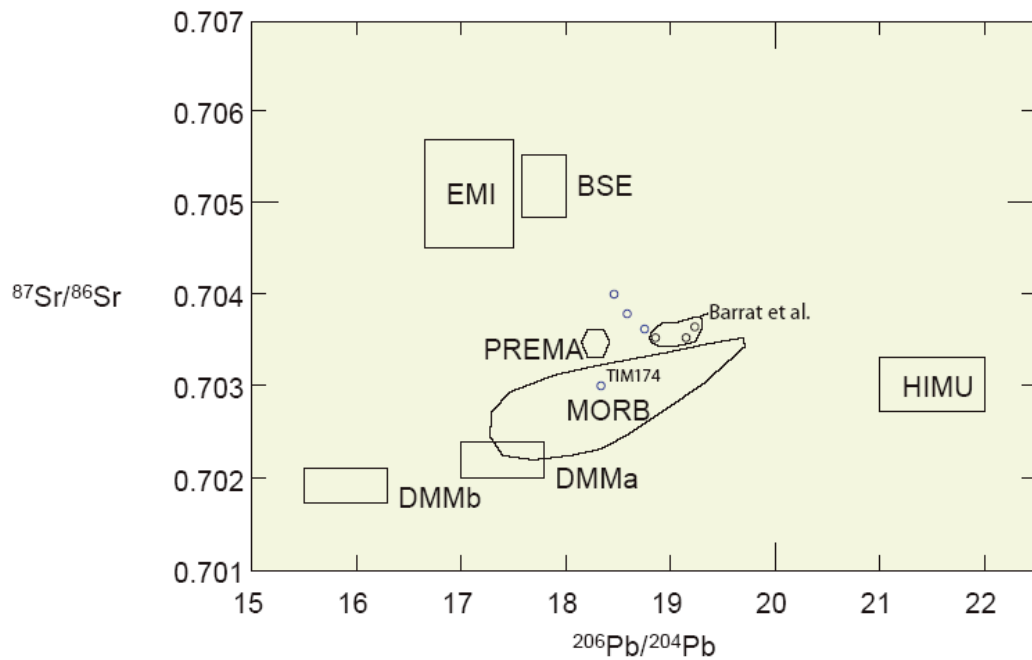


**Figure 2:** Simplified plate tectonic map of the Afar Triangle region showing the axes of spreading and the triple junction.

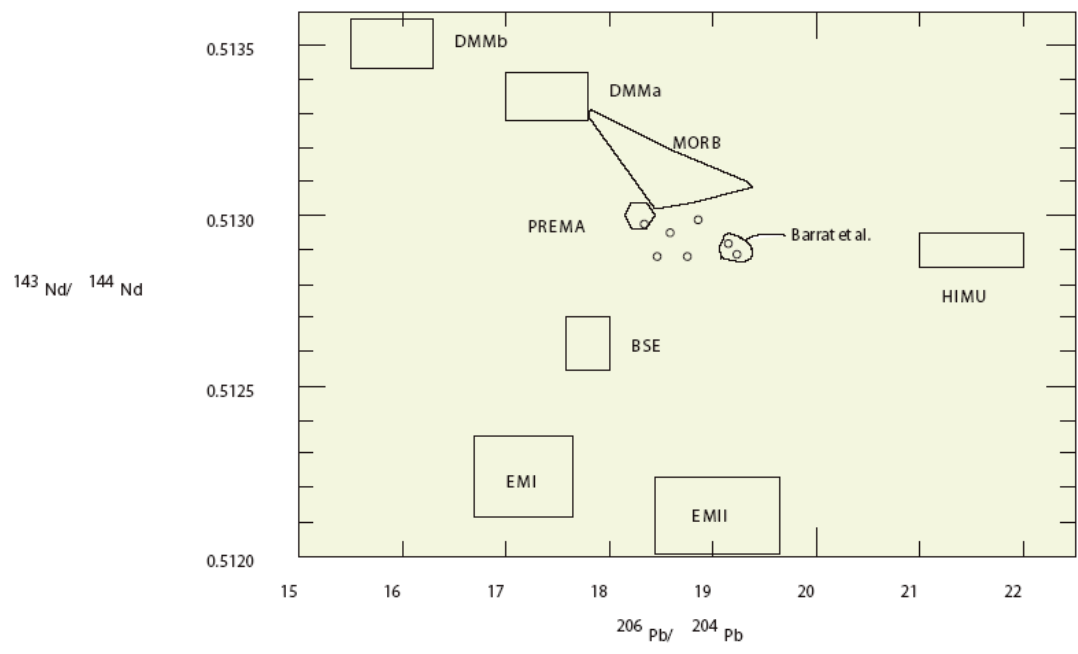
Image taken from: <http://wrgis.wr.usgs.gov/docs/geologic/jlwnstrn/alid/alidmaps.html>



**Figure 3:** Stable isotope ratio graph showing fields which represent various isotopically distinct mantle sources. Note the tight cluster formed by the data from Barrat et al. and this study.

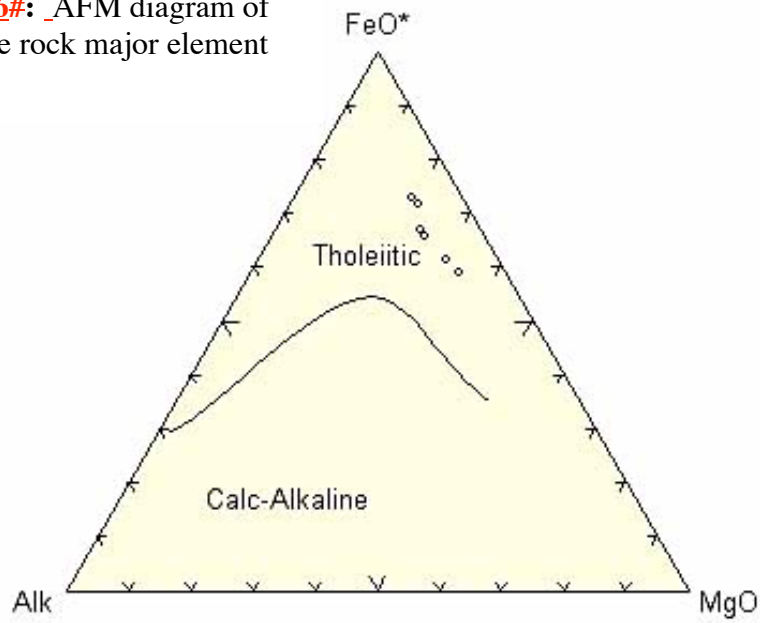


**Figure 4:** Stable isotope ratio graph showing fields which represent various isotopically distinct mantle sources. Note highland sample TIM-174 plots farthest from the cluster.

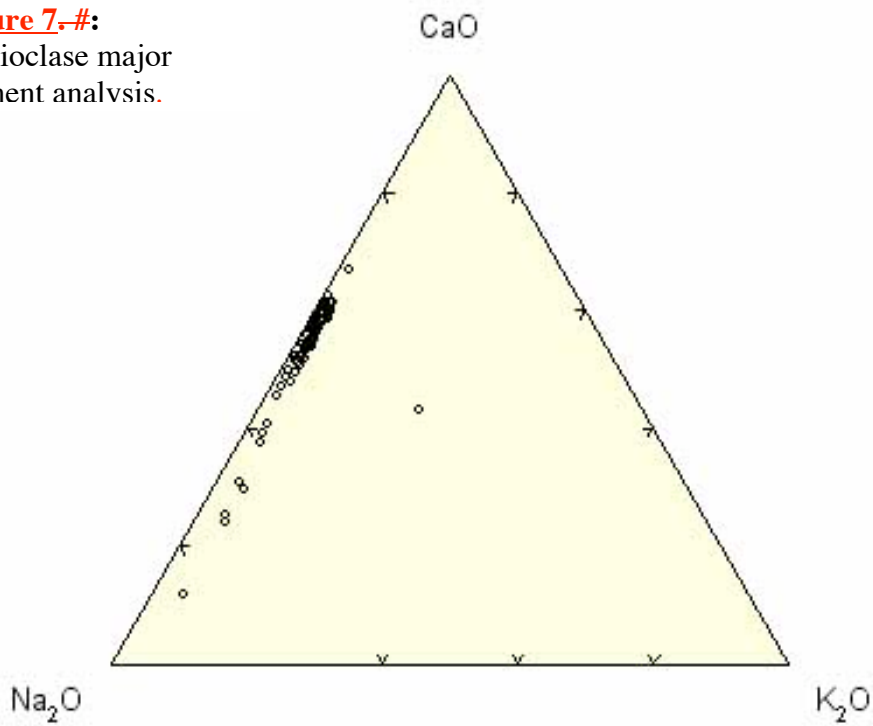


**Figure 5:** Stable isotope ratio graph showing fields which represent various isotopically distinct mantle sources.

**Figure 6#:** AFM diagram of the whole rock major element data.

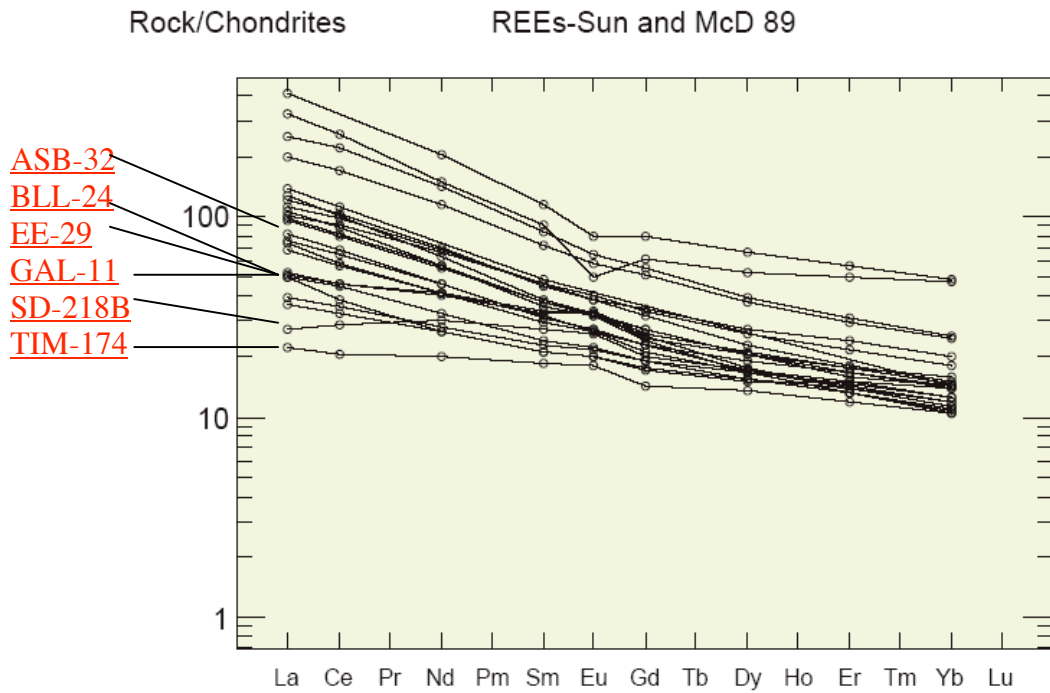
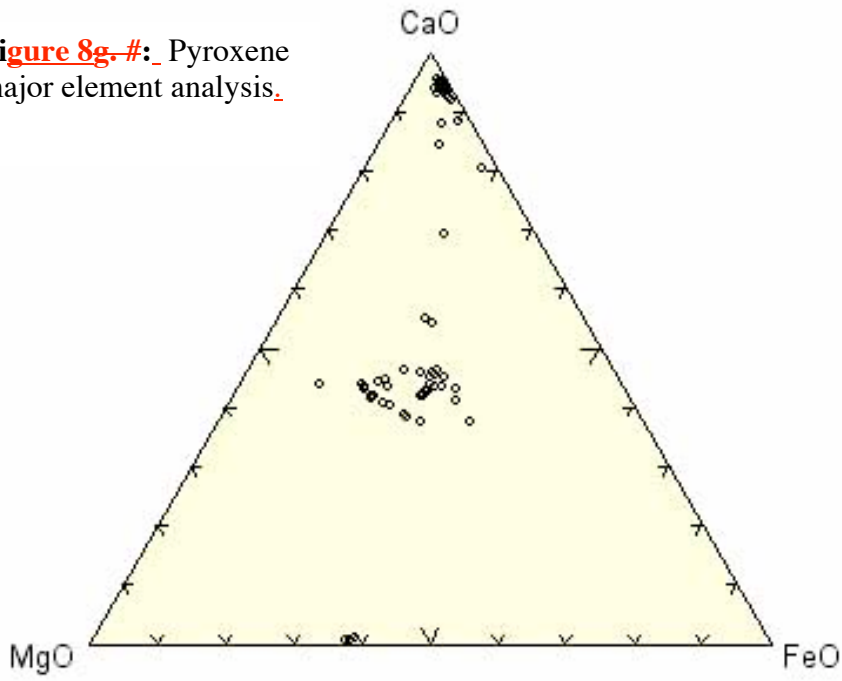


**Figure 7.#:** Plagioclase major element analysis.

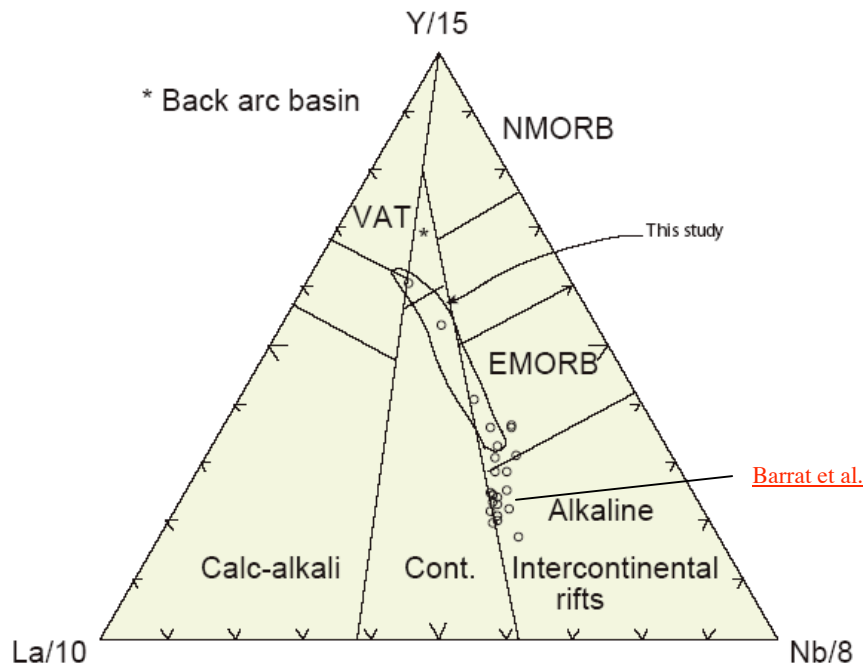




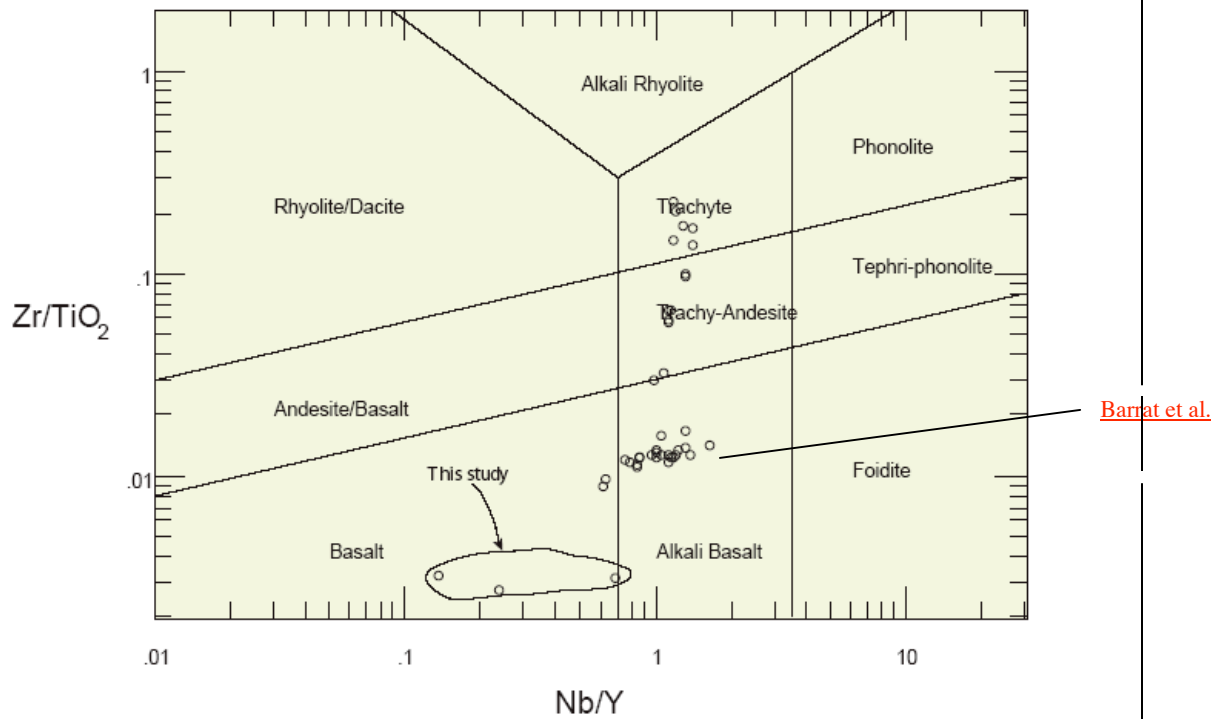
**Figure 8g-#:** Pyroxene major element analysis.



**Figure 9:** Rare earth element concentrations for the Erta' Ale samples and this study.

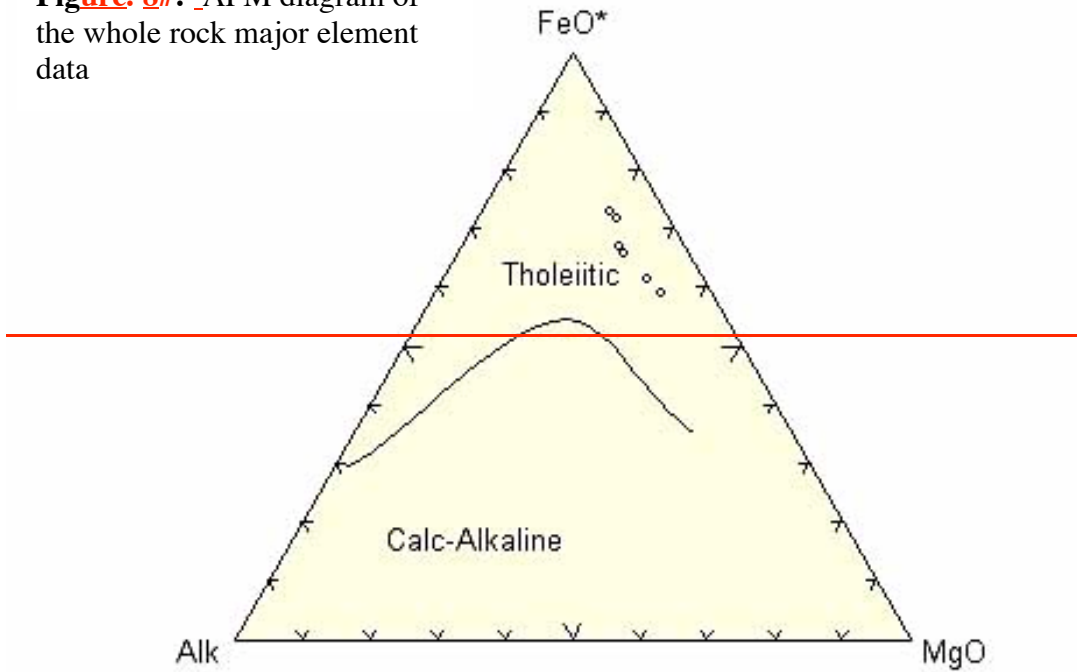


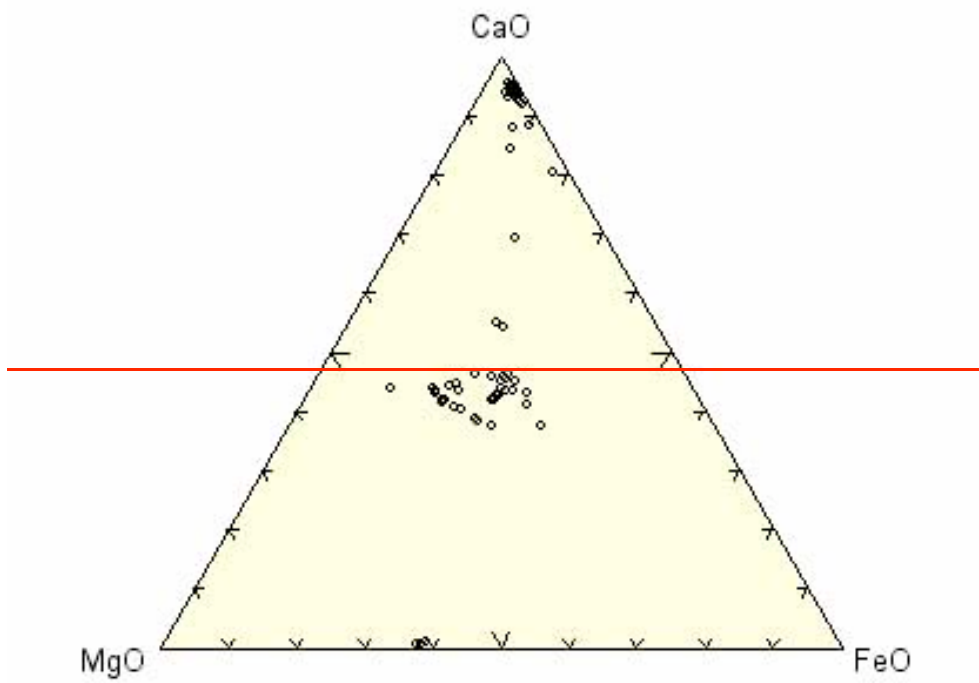
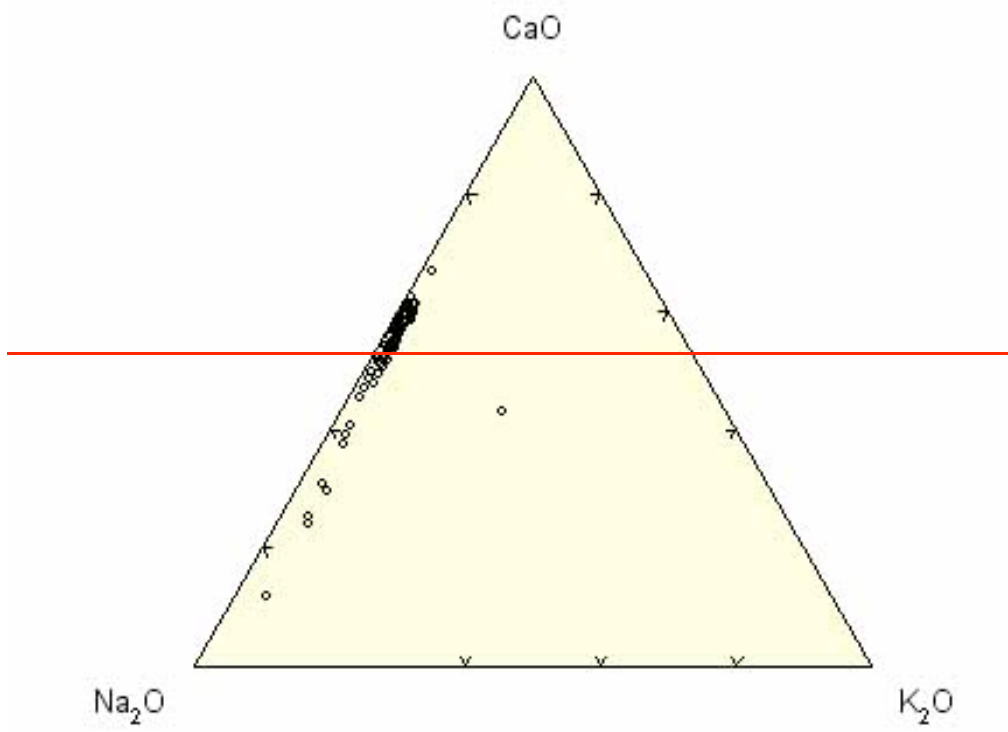
**Figure 10:** Tri-variant plot of La, Y, and Nb comparing data from Barrat and this study.



**Figure 11:** A plot of Nb/Y vs. Zr/TiO<sub>2</sub> reveals that several of the samples from this study are depleted in Zr, as compared to the Barrat et al. (1998) samples.

**Figure 8#:** AFM diagram of the whole rock major element data





Rock/Chondrites

REEs-Sun and McD 89

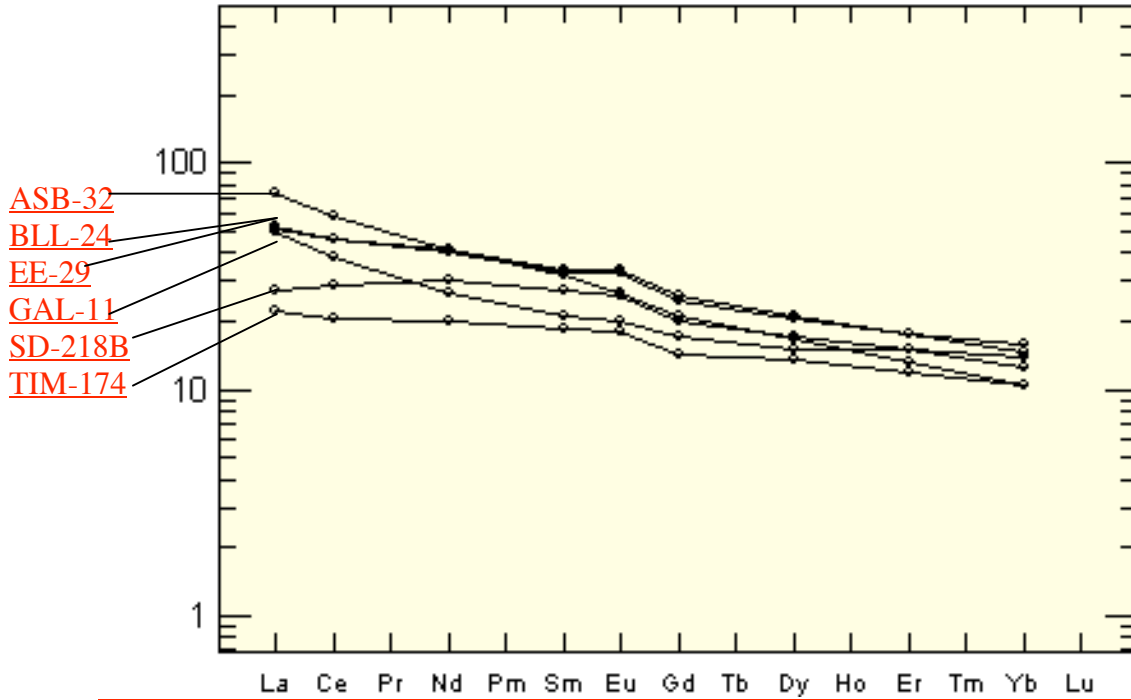


**Figure 12:** Rare earth element data for the six Afar samples. Going down from the highest La value, the REE trends represented are for site ASB-32, BLL-24, EE-29, GAL-11, SD-218B, and TIM-174.

Rock/NMORB

Sun/McDon. 1989-NMorb

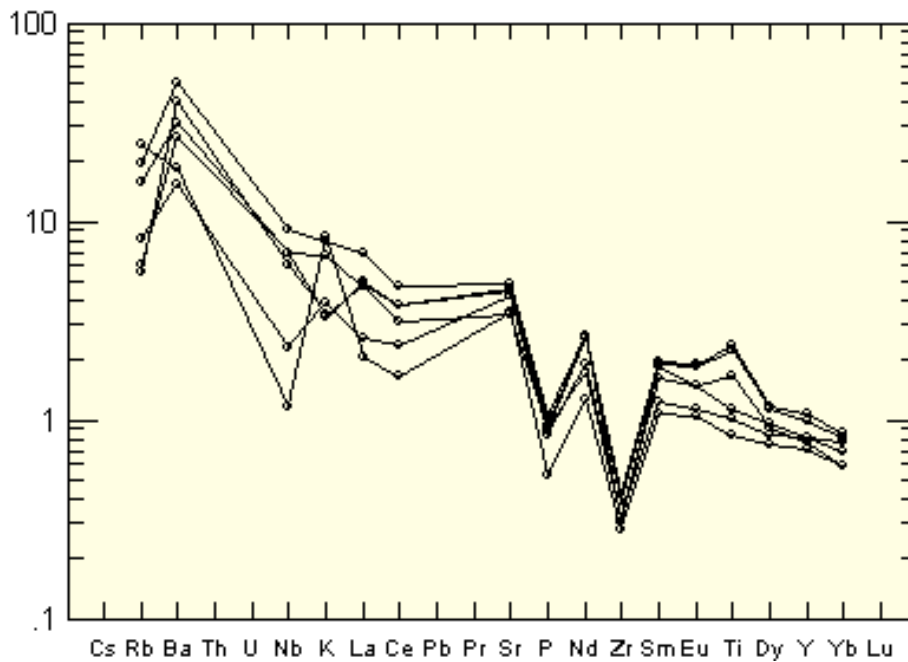


**Figure 13:** The REE data normalized to the NMORB trend does not fit very well.

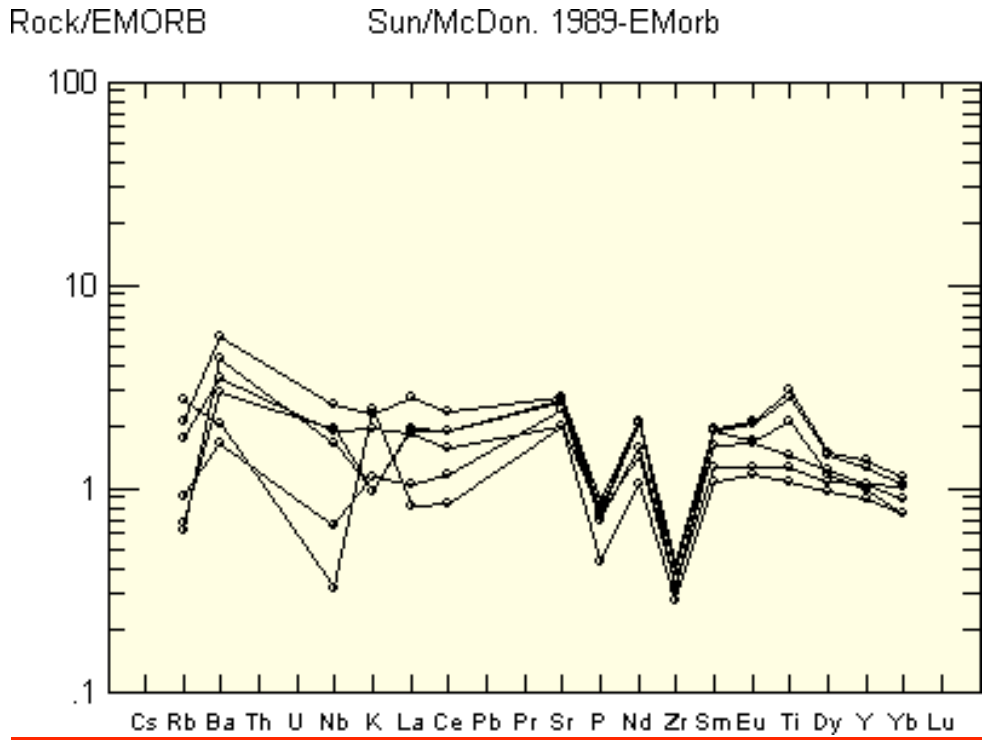


**Figure 14:** Normalizing to the EMORB trend seems to be the closest match.

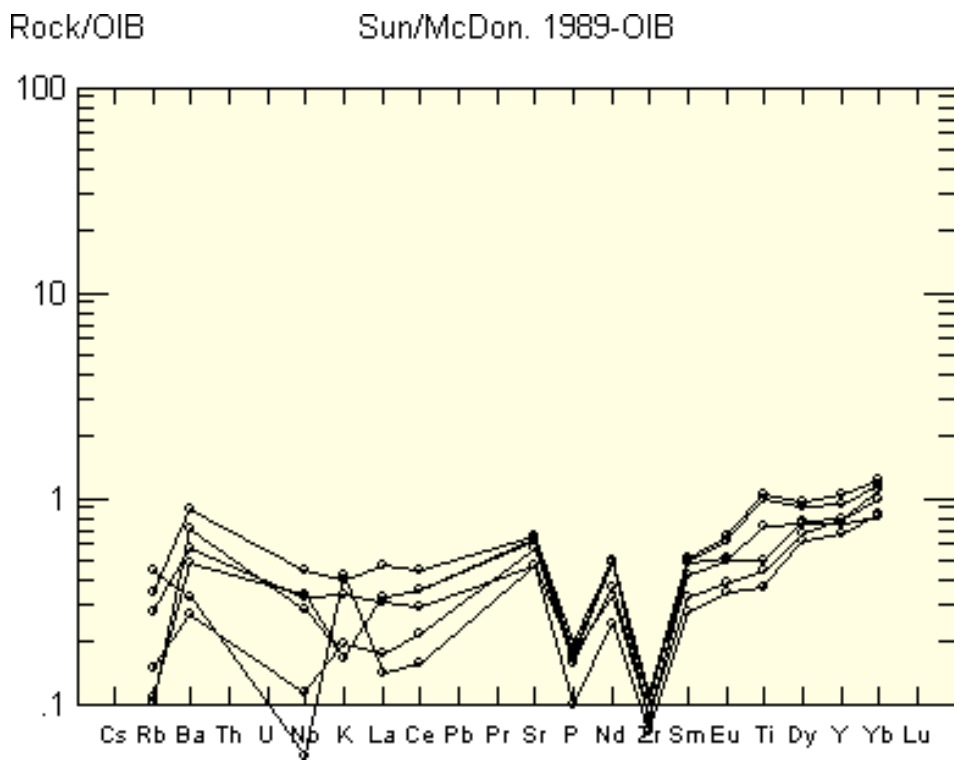


**Figure 15:** The REE data for the six samples normalized to the OIB trend yields many values that are too low.

## **CONCLUSIONS**

## **REFERENCES**

Barberi, F; Ferrara, G; Santacroce, R; Treuil, M; Varet, J. Transitional basalt-pantellerite sequence of fractional crystallization, Boina Center (Afar Rift, Ethiopia). JOURNAL OF PETROLOGY 16 (1): 22-56 1975.

Barrat, JA; Fourcade, S; Jahn, BM; Cheminée, JL; Capdevila, R. Isotope (Sr, Nd, Pb, O) and trace-element geochemistry of volcanics from the Erta' Ale range (Ethiopia). JOURNAL OF VOLCANOLOGY AND GEOTHERMAL RESEARCH 80: 85-100 1998.

Bixouard, H; Barberi, F; Varet, J. Mineralogy and petrology of Erta Ale and Boina volcanic series, Afar Rift, Ethiopia. JOURNAL OF PETROLOGY 21 (2): 401-436 MAY 1980.

Deer, W.A; Howie, RA; Zussman, J. An Introduction to the Rock-Forming Minerals. 2<sup>nd</sup> Edition. Harlow, England: Pearson Education Limited, 1992.

Frahm, Ellery E. Personal communication. Research Scientist/Manager, Electron \_\_\_\_\_ Microprobe Laboratory, Department of Geology and Geophysics, University of \_\_\_\_\_ MN, Twin Cities, MN.

Haileab, Bereket. Personal communication. Professor of Geology, Carleton College, Northfield, MN.

Kerr, Paul F. Optical Mineralogy. New York: McGraw-Hill Book Company. New York, 1959.

Winter, John D. An Introduction to Igneous and Metamorphic Petrology. Upper Saddle  
River, New Jersey: Prentice-Hall Inc, 2001.